

## A COLORIMETRIC AND FLUORESCENT CHEMOSENSOR OF $\text{Fe}^{3+}$ BASED ON AN ASYMMETRICAL SQUARYLIUM DYE

Min Lu<sup>1</sup>, Yue Wang<sup>1</sup>, Ying Li<sup>1</sup>, Zhongyu Li<sup>1,2\*</sup>, Song Xu<sup>1\*</sup>, Chao Yao<sup>1</sup>

<sup>1</sup> School of Petrochemical Engineering, Changzhou University, Jiangsu Key Laboratory of Advanced Catalytic Materials and Technology, Changzhou 213164, China

<sup>2</sup> Jiangsu Advanced Catalysis and Green Manufacturing Collaborative Innovation Center, Changzhou University, Changzhou 213164, China; e-mail: zhongyuli@mail.tsinghua.edu.cn; cyanine123@163.com

*A novel asymmetrical squarylium-dye-based dual signaling probe was synthesized and found to exhibit colorimetric and fluorescent properties on selective binding towards  $\text{Fe}^{3+}$  in ethanol/water (4:1, v/v) solution. The binding constant was determined to be  $7.69 \times 10^2 \text{ M}^{-1}$ , and the detection limit of SQ was  $9.158 \times 10^{-6} \text{ M}$ . Most importantly, the 1:2 stoichiometry of the host-guest complexation was confirmed by Job's method. Moreover, the high sensing ability of the receptor towards  $\text{Fe}^{3+}$  was also investigated by the electrochemical technique.*

**Keywords:** squarylium dye, iron ion (III), colorimetric sensor, fluorescent sensor.

## КОЛОРИМЕТРИЧЕСКИЙ И ФЛУОРЕСЦЕНТНЫЙ ХЕМОСЕНСОР $\text{Fe}^{3+}$ НА ОСНОВЕ АСИММЕТРИЧНОГО СКВАРИЛИЕВОГО КРАСИТЕЛЯ

M. Lu<sup>1</sup>, Y. Wang<sup>1</sup>, Y. Li<sup>1</sup>, Z. Li<sup>1,2\*</sup>, S. Xu<sup>1\*</sup>, C. Yao<sup>1</sup>

УДК 535.372;535.6

<sup>1</sup> Школа нефтехимической инженерии, Университет Чанчжоу, 213164, Чанчжоу, Китай

<sup>2</sup> Инновационный центр катализа и экологического производства, Университет Чанчжоу, 213164, Чанчжоу, Китай; e-mail: zhongyuli@mail.tsinghua.edu.cn; cyanine123@163.com

(Поступила 19 января 2017)

*Синтезирован зонд на основе нового асимметричного скварилиевого красителя, проявляющего колориметрические и флуоресцентные свойства при селективном связывании с  $\text{Fe}^{3+}$  в растворе этанола с водой (в пропорции 4:1). Для данного красителя определены константа связывания  $7.69 \times 10^2 \text{ M}^{-1}$  и предел обнаружения  $9.158 \times 10^{-6} \text{ M}$ . Стехиометрия 1:2 при связывании красителя подтверждена методом Джоба. С помощью электрохимического метода показана высокая чувствительность к наличию  $\text{Fe}^{3+}$ .*

**Ключевые слова:** скварилиевый краситель,  $\text{Fe}^{3+}$ , колориметрический сенсор, флуоресцентный сенсор.

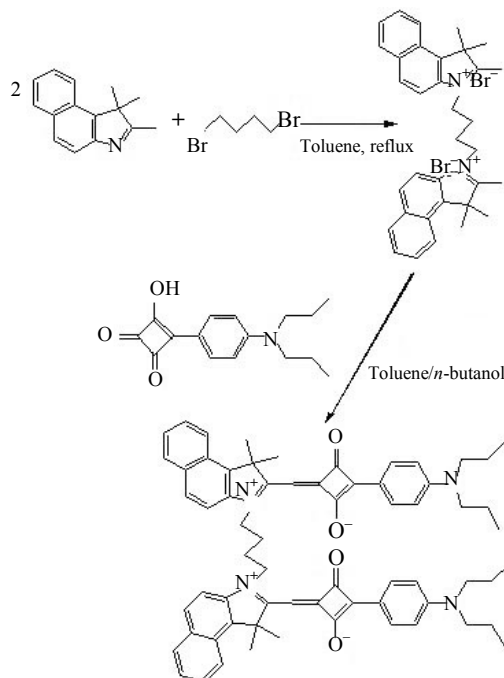
**Introduction.** The design of chromogenic and fluorescent chemosensors for the selective detection of cations, especially for metal ions, has always been of particular significance due to their potential applications in such fields as chemistry, biology, medicine, and ecology [1–3]. In recent years, fluorescent chemosensors capable of collectively recognizing cations have attracted much attention because of their potential application in environmental and medical research [4–8]. Among heavy metals, iron not only becomes the most common trace element but also performs a major function in the cells of all systems of the organism as well as in various cellular biochemical processes [9]. Especially,  $\text{Fe}^{3+}$  plays a major role in biochemical processes at the cellular level. However, high levels of  $\text{Fe}^{3+}$  in the body are commonly associated with increasing risk of certain cancers and dysfunction of the heart, pancreas, and liver [10, 11]. As a consequence, many methods have been proposed to measure trace amounts of iron ions, including atomic absorption, ICP atomic emission, UV-vis absorption, and fluorescence spectroscopy. Resulting from its high sensitivity and

facile operation, fluorescence spectroscopy is widely employed. While iron belongs to heavy transition-metal ions, which quench fluorescence emission via enhanced spin-orbital coupling energy or electron transfer, only a few fluorescent chemosensors for detecting iron ions have been reported up to the present. In conclusion, the development of highly selective chemosensors for iron remains a challenge.

Herein, we have designed a novel colorimetric and fluorescent chemosensor of  $\text{Fe}^{3+}$  based on an asymmetrical squarylium dye. Such a squaraine chemosensor exhibited remarkably high sensitivity and reversibility for sensing iron ions in ethanol/water (4:1, v/v) solution.

**Experimental.** All the chemicals were purchased from Shanghai Chemical Reagents Company (China) and were used without further purification. Nitrates ( $\text{Na}^+$ ,  $\text{Cd}^{2+}$ ,  $\text{K}^+$ ,  $\text{Mg}^{2+}$ ,  $\text{Ca}^{2+}$ ,  $\text{Al}^{3+}$ ,  $\text{Cr}^{3+}$ ,  $\text{Zn}^{2+}$ ,  $\text{Fe}^{3+}$ ,  $\text{Cu}^{2+}$ ,  $\text{Pb}^{2+}$ ,  $\text{Co}^{2+}$ ,  $\text{Ni}^{2+}$ , and  $\text{Ba}^{2+}$ ) were used as the metal cations source spectroscopy. The pH was measured with a Mettler Toledo MP220 digital pH meter. The infrared spectra were obtained on a Protégé 460 spectrometer, using KBr discs.  $^1\text{H}$  NMR,  $^{13}\text{C}$  NMR spectra were obtained on a Bruker Avance III 300 MHz NMR using DMSO as the solvent and tetramethylsilane (TMS) as the internal standard. Mass spectral studies were carried out using an LCMS-2020 mass spectrometer by passing the LC step. UV-vis spectra were obtained in a 1 cm path length quartz cell using a UV-759 spectrophotometer in ethanol/water (4:1, v/v) solution. Fluorescence emission spectra were recorded on an F-280 spectrometer. Electrochemical experiments were recorded in 0.5 M  $\text{H}_2\text{SO}_4$  solution using an LK98BII electrochemical analyzer (Lanlike Ltd., China) with a 50 mV/s scan rate. The morphologies of the samples were characterized by field-emission scanning electron microscopy (FE-SEM, JEOL, JSM-6360LA).

**Synthesis of the asymmetrical squarylium dye.** The synthesis route of the asymmetrical squarylium dye is shown in Scheme 1. First, N-butyl disubstituted 2,3,3-trimethylnaphtho[1,2-d] (NTP) was synthesized as follows: a 250 mL three-neck round bottom flask was equipped with a temperature probe, a magnetic stirrer, and a nitrogen inlet adaptor with a condenser, where 12.2220 g of 2,3,3-trimethylnaphtho[1,2-d]pyrrole, 5.4000 g 1,4-dibromobutane, and 30 mL of toluene were refluxed for 36 h with  $\text{N}_2$ . After cooling to room temperature, the product was collected by filtration. The crude product was further purified by a silica gel solid phase and an eluent consisting of petroleum ether/ethyl acetate (1:4, v/v) and dried in a vacuum to give a yield of 68.7% as a gray solid.



Scheme 1. Synthesis of N-butyl disubstituted-2,3,3-trimethylnaphtho[1,2-d] (NTP) and asymmetrical squarylium dye (SQ).

The asymmetrical squarylium (SQ) chemosensor was readily prepared by one-step condensation of NTP (0.1222 g, 0.2198 mmol) and 3-[4-(N,N-dibutylamino)-phenyl]-4-hydroxycyclobutene-1,2-dione (0.1224 g, 0.4112 mmol) in 20 mL of *n*-butanol and 20 mL of toluene. The mixture was refluxed for 8 h with  $\text{N}_2$  and

the azeotropic removal of water. After being cooled to room temperature, the blue precipitate was filtered to form 0.139 g of SQ (64%). FTIR (KBr): 1561.44 (benzene ring vibration), 2923.80, 2852.18, 1334.43 (CH<sub>2</sub>, CH<sub>3</sub>), 819.85, 745.11 (the *para* position of the benzene ring). <sup>1</sup>H NMR (300 MHz, DMSO)  $\delta$  (ppm): 0.89 (dd,  $J = 22.8$ ,  $J = 15.6$  Hz, 6H, -CH<sub>3</sub>), 1.04 (t,  $J = 6.8$  Hz, 6H, -CH<sub>3</sub>), 1.22 (s, 16H), 1.40–2.01 (m, 12H, -CH<sub>3</sub>), 4.74 (d,  $J = 7.2$  Hz, 4H, -CH<sub>2</sub>-), 5.32 (s, 4H, -CH<sub>2</sub>-), 6.16 (s, 2H, -CH=), 6.67–8.43 (m, 20H). <sup>13</sup>C NMR (300 MHz, DMSO)  $\delta$  (ppm): 209.12, 186.42, 185.44, 182.54, 181.67, 167.90, 150.88, 137.96, 134.19, 132.55, 131.86, 130.60, 130.46, 129.98, 129.07, 128.94, 127.54, 124.95, 122.12, 113.11, 111.73, 89.88, 54.39, 52.86, 51.75, 48.71, 29.71, 29.33, 27.22, 26.94, 24.93, 20.63, 11.40. MS (ESI):  $m/z = 983.10$ ,  $m/z_{\text{calc}} = 983.24$  for C<sub>66</sub>H<sub>70</sub>N<sub>4</sub>O<sub>4</sub>.

**General UV-vis and fluorescence titration experiments.** All titration experiments were obtained at room temperature. Stock solutions ( $1 \times 10^{-2}$  M) of the metal ions Na<sup>+</sup>, Cd<sup>2+</sup>, K<sup>+</sup>, Mg<sup>2+</sup>, Ca<sup>2+</sup>, Al<sup>3+</sup>, Cr<sup>3+</sup>, Zn<sup>2+</sup>, Fe<sup>3+</sup>, Cu<sup>2+</sup>, Pb<sup>2+</sup>, Co<sup>2+</sup>, Ni<sup>2+</sup>, and Ba<sup>2+</sup> in distilled water were prepared. Compound SQ was dissolved in ethanol/water (4:1, v/v) at room temperature to provide the probe stock solution ( $1 \times 10^{-5}$  M). Test solutions were prepared by placing 3 mL of the sensor stock solution into a cuvette and adding 0.05 mL of each metal ion. After shaking them well for a few seconds, the absorption and emission spectra were recorded.

**Results and discussion.** *UV-vis and fluorescence spectral responses.* In recent years, selectivity has become a crucial criterion to evaluate whether the chemosensor is an excellent probe [12]. Furthermore, highly selective recognition of the target ion from various cations has emerged as an attractive tool due to its wide applications in diverse areas and impact on the environment [13]. Thus, high selectivity is usually required for the chemosensor to accomplish detection. A clear and selective color change from blue to yellow-green was observed with the addition of Fe<sup>3+</sup>. The response of SQ towards various cations analytes was evaluated with UV-visible and fluorescence spectroscopic techniques. Figure 1 shows the absorption and fluorescence spectra of SQ ( $1 \times 10^{-5}$  M), which were studied in ethanol/water (4:1, v/v) upon addition of various metal ions such as Na<sup>+</sup>, Cd<sup>2+</sup>, K<sup>+</sup>, Mg<sup>2+</sup>, Ca<sup>2+</sup>, Al<sup>3+</sup>, Cr<sup>3+</sup>, Zn<sup>2+</sup>, Fe<sup>3+</sup>, Cu<sup>2+</sup>, Pb<sup>2+</sup>, Co<sup>2+</sup>, Ni<sup>2+</sup>, and Ba<sup>2+</sup> ( $1 \times 10^{-2}$  M). In Fig. 1a, upon addition of a constant amount (0.05 mL) of Fe<sup>3+</sup> ions to SQ, a significant decrease in absorbance at 640 nm was observed, and the addition of other metal ions (Cd<sup>2+</sup>, Co<sup>2+</sup>, Pb<sup>2+</sup>, Al<sup>3+</sup>, Na<sup>+</sup>, Ni<sup>2+</sup>, Mg<sup>2+</sup>, K<sup>+</sup>, Cr<sup>3+</sup>, Zn<sup>2+</sup>, Ca<sup>2+</sup>, and Ba<sup>2+</sup>) to the solution did not result in any drastic absorbance change. Furthermore, there was no significant change in the solution color of SQ upon addition of these metal ions. These results demonstrated our expectation that a small change of the substituent on the receptor may result in a significant change of the sensing properties of the receptor.

The above absorption results encouraged us to explore the fluorescence changes of the SQ dye in the metal complex form. We chose the same metal ions used for the fluorescence studies: Pb<sup>2+</sup>, Al<sup>3+</sup>, Na<sup>+</sup>, Ni<sup>2+</sup>, Mg<sup>2+</sup>, K<sup>+</sup>, Cr<sup>3+</sup>, Zn<sup>2+</sup>, Ca<sup>2+</sup>, Ba<sup>2+</sup>, Cu<sup>2+</sup>, and Fe<sup>3+</sup> in ethanol/water (4:1, v/v). As shown in Fig. 1b, the emission spectrum of SQ was perturbed in the presence of Fe<sup>3+</sup> ions, whereas no significant change was observed with other metal ions. The emission quenching arises from the static quenching process, which involved the interaction of the fluorogenic quinoline moiety of SQ with Fe<sup>3+</sup> ions. The selective quenching of SQ also suggested that Fe<sup>3+</sup> was coordinated to the heteroatom-N of SQ, which acted as donor sites [14–16]. Moreover, among the tested metal ions, Fe<sup>3+</sup> (0.05 mL) induced a blue shift, increasing slightly from 681 nm to 680 nm.

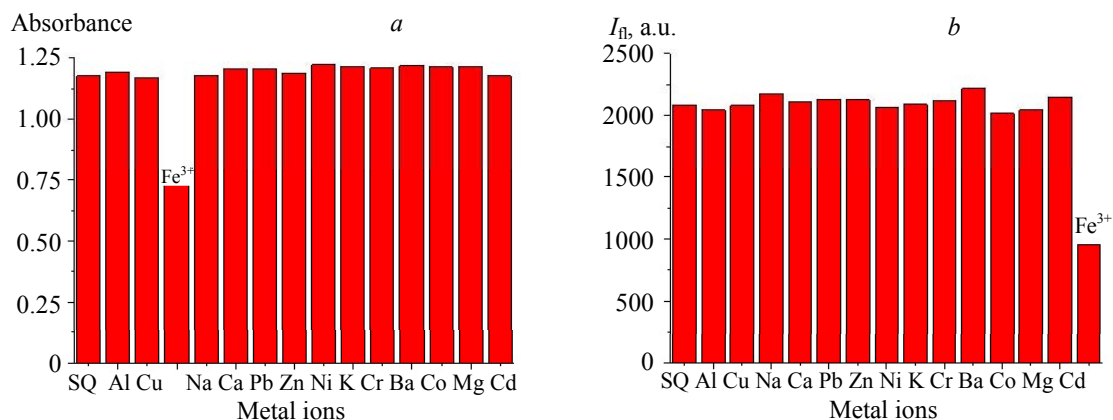


Fig. 1. Absorption (a) and fluorescence (b) spectra of SQ ( $1 \times 10^{-5}$  M) in the presence of different metal ions (0.01 M) in ethanol/water (4:1).

Therefore, the chemosensor has a better selectivity for  $\text{Fe}^{3+}$  over the other cations tested under the same conditions. Complex formation with a cation leads to hypsochromic shifts of both absorption and emission spectra due to the interaction of the cation with the lone electron pair of the nitrogen atom involved in the chromophoric system of the dye molecule.

**Spectral titration and detection limit experiment.** To evaluate the sensing behavior of the SQ dye towards  $\text{Fe}^{3+}$ , the titration of the SQ dye with  $\text{Fe}^{3+}$  has been carried out for absorption and emission spectra in ethanol/water (4:1, v/v). We chose the same metal ions used for the previous studies, such as  $\text{Pb}^{2+}$ ,  $\text{Al}^{3+}$ ,  $\text{Na}^+$ ,  $\text{Ni}^{2+}$ ,  $\text{Mg}^{2+}$ ,  $\text{K}^+$ ,  $\text{Cr}^{3+}$ ,  $\text{Zn}^{2+}$ ,  $\text{Ca}^{2+}$ ,  $\text{Ba}^{2+}$ ,  $\text{Cu}^{2+}$ , and  $\text{Fe}^{3+}$  in ethanol/water (4:1, v/v). As shown in Fig. 2, upon addition of  $\text{Fe}^{3+}$ , the intensity of the original absorption band at 640 nm gradually decreased and the color changed from blue to yellow-green. When the concentration of  $\text{Fe}^{3+}$  ion was up to 1.34 mM, no obvious absorption at 640 nm was exhibited. This may have been due to the changes of the molecular orbitals resulting from the complexation of  $\text{Fe}^{3+}$  with the heteroatom-N of the SQ unit. Moreover, Fig. 2 shows the Benesi-Hilderbrand plots of SQ with  $\text{Fe}^{3+}$ . A good linearity between  $[A_0/(A_0 - A)]$  and the concentration of  $\text{Fe}^{3+}$  was obtained. The measured absorbance  $[A_0/(A_0 - A)]$  at 640 nm shows a linear relationship with a change of  $1/[\text{Fe}^{3+}]$  ( $R = 0.95961$ ). The association constant  $K_a$  of SQ and  $\text{Fe}^{3+}$  in ethanol/water (4:1, v/v) was evaluated to be  $769 \text{ M}^{-1}$ .

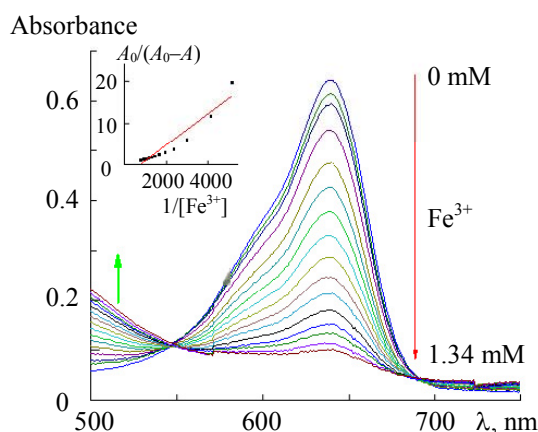


Fig. 2. Changes of absorption spectrum about SQ ( $1.0 \times 10^{-5} \text{ M}$ ) in ethanol/water (4:1, v/v) solution upon addition of  $\text{Fe}^{3+}$  (0–1.34 mM), Inset: Benesi-Hilderbrand plots of SQ with  $\text{Fe}^{3+}$ .

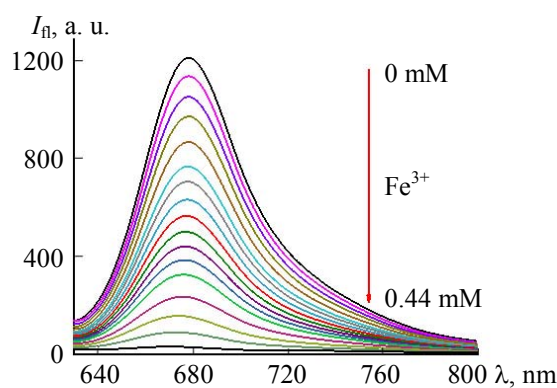


Fig. 3. Fluorescence spectra, exhibition of SQ ( $1.0 \times 10^{-5} \text{ M}$ ) with gradual addition of different amounts of  $\text{Fe}^{3+}$  (0–0.44 mM).

Furthermore, the titration studies for emission spectra to evaluate the sensing behavior of the SQ dye with  $\text{Fe}^{3+}$  metal ions were also performed. As shown in Fig. 3, as the concentration of  $\text{Fe}^{3+}$  increased, the intensity in the emission peak of SQ gradually decreased, and the emission peak intensity approximately decreased to 0 with a slight blue-shift to 675 nm when the  $\text{Fe}^{3+}$  concentration reached  $4.4 \times 10^{-4} \text{ M}$ . This result can be reasonably assigned to the coordination of  $\text{Fe}^{3+}$  to the ligand of SQ. The deprotonation of the heteroatom-N of SQ allowed the charge transfer from the ligand to  $\text{Fe}^{3+}$ , which caused the fluorescence quenching behavior of ligands upon  $\text{Fe}^{3+}$  complexation.

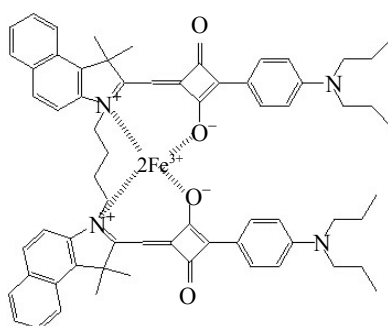
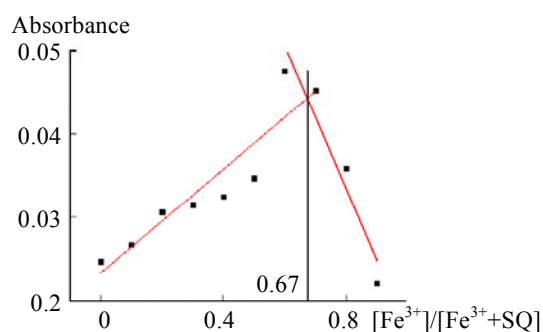
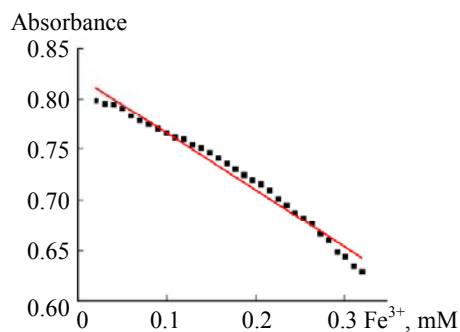
The stoichiometry of the SQ complex was further determined by Job's plot (Fig. 4). The absorbance intensity at 640 nm went through a maximum when the mole fraction of  $\text{Fe}^{3+}$  was 0.66, which indicated that a 1:2 stoichiometry was the most possible binding mode of SQ and  $\text{Fe}^{3+}$  (Scheme 2). As shown in Fig. 5, 32 sets of experimental data were selected to plot the linearity of the  $\text{Fe}^{3+}$  concentration and absorbance. Each set was dropped with the equal  $\text{Fe}^{3+}$  of  $5 \times 10^{-4} \text{ mol}$ , and the result of the analysis is as follows:

$$Y = -0.56525X + 0.82261, \quad (1)$$

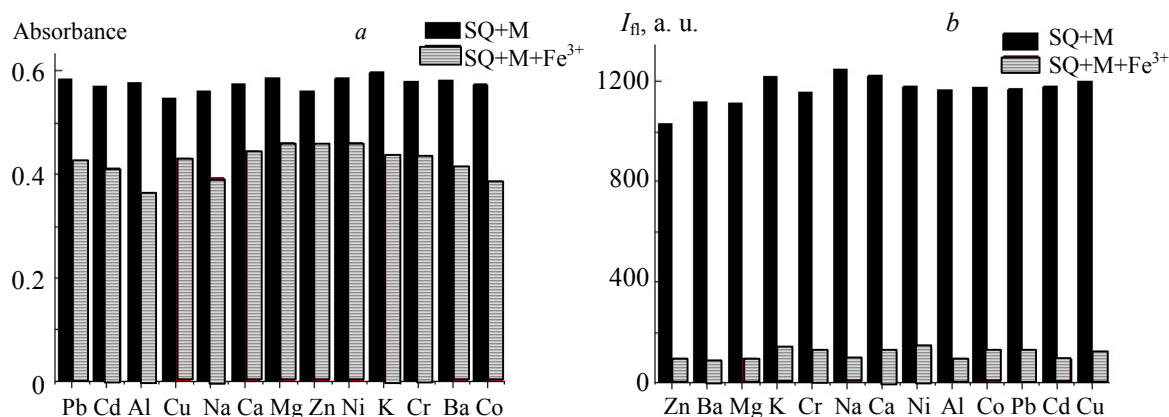
$$\delta = \sqrt{\sum (A_0 - \bar{A}_0)^2 / (N - 1)}, \quad (2)$$

$$\text{LOD} = K\delta/S. \quad (3)$$

The value of  $\delta$  represents the standard deviation of the absorbance.  $S$  is the absolute value of the line's slope, and the  $K$  is constant ( $K = 3$ ). As a result, the detection limit of  $\text{Fe}^{3+}$  was evaluated to be  $9.158 \times 10^{-6} \text{ M}$ .

Scheme 2. Proposed complexation mechanism of SQ with  $\text{Fe}^{3+}$ .Fig. 4. Job's plots of the complexation between  $\text{SQ-Fe}^{3+}$  in ethanol/water (4:1), the total concentration of SQ and  $\text{Fe}^{3+}$  is  $2 \times 10^{-5}$  mol/L.Fig. 5. Plot of the absorbance at 641 nm for  $\text{SQ-Fe}^{3+}$  in ethanol/water (4:1, v/v) from 9.99 to 319.46  $\mu\text{M}$ .

One challenge for the chemosensor was to achieve the specific detection of  $\text{Fe}^{3+}$  in the presence of a wide range of potentially competing ions because the system might exhibit cross-sensitivity towards other metal ions. Therefore, competitive experiments of the background metal ions with  $\text{Fe}^{3+}$  were also conducted (Fig. 6). It was found that the competitive cations did not induce observable change in the absorption and fluorescence spectra.

Fig. 6. Changes in the absorption (a) and fluorescence intensity (b) of SQ ( $1.0 \times 10^{-5}$  M) to  $\text{Fe}^{3+}$  in the presence of various competitive ions (1 mL) in ethanol/water (4:1, v/v).

**Reversibility of the binding of  $\text{Fe}^{3+}$  by SQ.** Reversible usage was an important feature for optical chemosensors, which allowed improvement of on-off sensors and decreased the analysis cost. We carried out studies on the reversibility of the sensor to investigate whether the chemical probe could be reused. As seen in Fig. 7, upon addition of 0.05 mL of EDTA ( $1.0 \times 10^{-2}$  M) into the solution of the  $\text{SQ-Fe}^{3+}$  complex, the solution did not return to the metal-free spectrum. However, the addition of EDTA resulted in partial reversibi-

lity in the absorption spectrum. This indicated that the chelating ability of the EDTA and  $\text{Fe}^{3+}$  is higher than that of SQ and  $\text{Fe}^{3+}$ . As a result, the present sensor could be appropriate to construct an on-off  $\text{Fe}^{3+}$  sensor repeatedly.

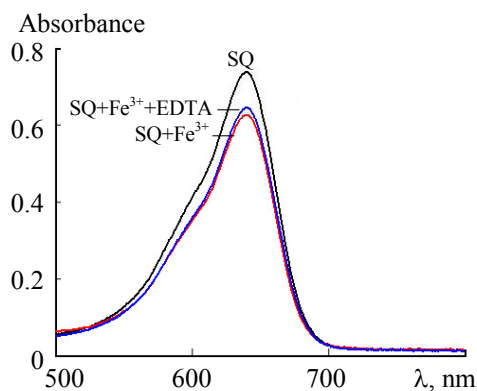


Fig. 7. UV-vis absorption of SQ ( $1.0 \times 10^{-5}$  M) in the presence of  $\text{Fe}^{3+}$  (0.05 mL) with EDTA (0.05 mL) in ethanol/water (4:1, v/v).

*Influence of the pH on SQ.* The pH value of the environment around the probe usually shows an effect on its performance towards the target metal ion due to the protonation or deprotonation for the chromophoric and hydrolysis reaction for the metal ions in the basic condition. To study the influence of the pH to SQ, pH absorption titrations of SQ were performed in an ethanol/water (4:1, v/v) system at a probe concentration of 10  $\mu\text{M}$ . Experimental results showed that when the pH increased from 6.66 to 11.54 (Fig. 8a), the absorption band at 640 nm decreased sharply. Furthermore, a notable color change from blue to almost light green was observed when the pH value increased. However, as shown in Fig. 8b (in an acidic environment), when the pH value decreased from 6.66 to 2.00, the absorption band at 640 nm decreased slowly with a notable color change from blue to orange. The results confirm that SQ was more sensitive to  $\text{OH}^-$  than  $\text{H}^+$ .

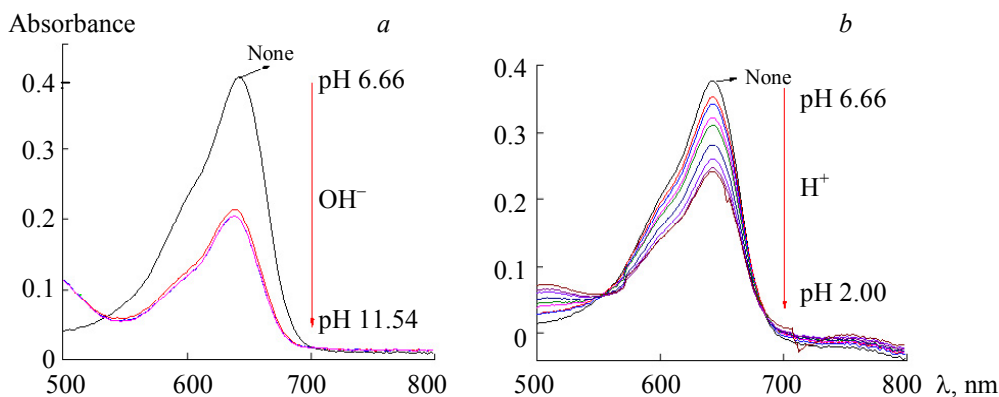


Fig. 8. UV-vis absorption spectra of SQ ( $1.0 \times 10^{-5}$  M) in ethanol/water (4:1, v/v) at different pH values (a) (6.66–11.54), (b) (2.00–6.66).

*Mechanistic studies of the chemosensor SQ.* The results (Fig. 9) of the study of the electrochemical properties of SQ and SQ- $\text{Fe}^{3+}$  showed that there were no oxidation and reduction peaks when SQ was kept in 0.5 M  $\text{H}_2\text{SO}_4$  solution. In the presence of 0.2 mL of  $\text{Fe}^{3+}$ , the reduction peak changed significantly in a dramatic negative shift from 0.2 to 0.4 V, and a dramatic negative shift of the oxidation peak of SQ from 0.5 to 0.6 V was also observed. The changes in the volt-amperometric behavior of SQ might arise from the incorporation of  $\text{Fe}^{3+}$  ions, which caused some structural changes of SQ.

To gain an understanding of the structures of the SQ-Fe<sup>3+</sup> complex, the binding mode between SQ and Fe<sup>3+</sup> was studied using the <sup>1</sup>H NMR spectrum (Fig. 10). The <sup>1</sup>H NMR spectrum of SQ in DMSO showed 20 aromatic protons at 8.43–6.67 ppm [20H], 6.16 ppm [2H, –CH=], 5.32 ppm [4H, –CH<sub>2</sub>–], and 4.74 ppm [4H, –CH<sub>2</sub>–]. After coordination with Fe<sup>3+</sup>, all of the peaks moved to lower field, and then the peaks at 7.40, 7.49, 7.83 and 7.89 ppm disappeared, demonstrating the coordination process between the SQ group and Fe<sup>3+</sup> along with the electronic structural change of SQ. The absorption-based Job's plot showed that the maximum absorption occurred when the mole fraction of Fe<sup>3+</sup> reached 0.5, which indicates the 1:2 binding mode between SQ and Fe<sup>3+</sup>. The proposed complexation mechanism of SQ with Fe<sup>3+</sup> and Ag<sup>+</sup> is shown in Scheme 2.

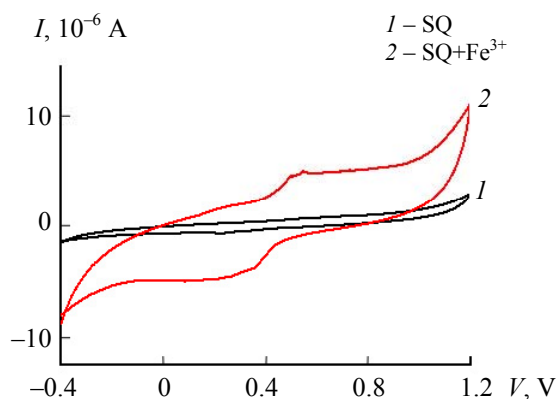


Fig. 9. Changes in the voltammetric behaviors of SQ solution ( $2.0 \times 10^{-5}$  M) in ethanol/water (4:1, v/v) upon addition of Fe<sup>3+</sup> (0.2 mL,  $v = 50$  mV/s).

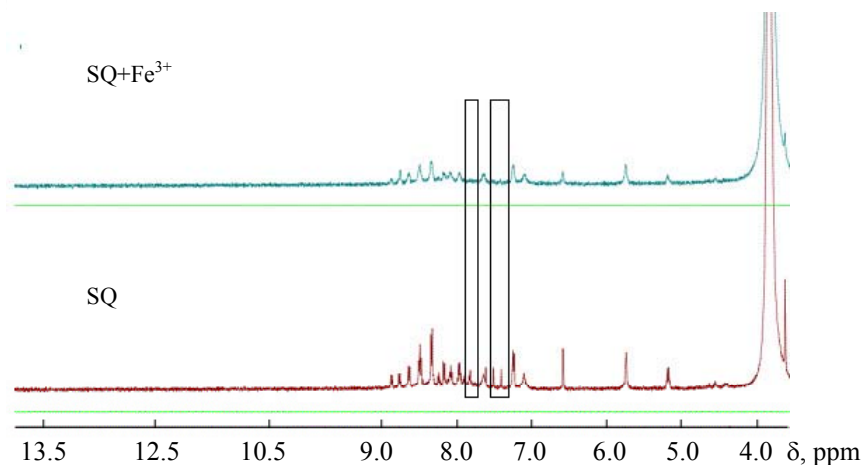


Fig. 10. <sup>1</sup>H NMR spectra of SQ, SQ-Fe<sup>3+</sup> in DMSO (Note: for the complex, 1.0 equiv of Fe<sup>3+</sup> was added to the SQ).

**Conclusion.** We have designed and synthesized a dual-mode sensor based on an asymmetrical squarylium dye for the detection of Fe<sup>3+</sup> in ethanol/water (4:1, v/v). The chemosensor can be immediately utilized for the detection of Fe<sup>3+</sup> in the presence of other competitive metal ions by both colorimetric and fluorescent change.

**Acknowledgment.** This work was financially supported by the Natural Science Foundation of Jiangsu Province, China (BK20150259) and the Natural Science Foundation of Changzhou City, China (CJ20140053).

## REFERENCES

1. X. W. Cheng, Y. Zhou, Y. Fang, Q. Q. Rui, C. Yao, *RSC Adv.*, **5**, 19465–19469 (2015).
2. S. Wang, T. Cong, Q. Liang, Z. Li, S. Xu, *Tetrahedron*, **71**, 5478–5483 (2015).
3. S. Ye, Q. Liang, Z. Li, S. Xu, C. Yao, *Tetrahedron*, **73**, 1350–1357 (2017).
4. Q. Lin, Y. P. Fu, P. Chen, T. B. Wei, Y. M. Zhang, *Dye. Pigm.*, **96**, 1–6 (2013).
5. X. H. Cheng, S. Li, A. S. Zhong, J. Q. Qin, Z. Li, *Sens. Actuators B*, **157**, 57–63 (2011).
6. J. Y. Choi, D. Kim, J. Yoon, *Dyes Pigm.*, **96**, 176–179 (2013).
7. S. J. Kim, J. Y. Noh, K. Y. Kim, J. H. Kim, H. K. Kang, S. W. Nam, S. H. Kim, S. S. Park, C. Kim, J. H. Kim, *Inorg. Chem.*, **51**, 3597–3602 (2012).
8. M. Z. Tian, X. J. Peng, J. L. Fan, J. Y. Wang, S. G. Sun, *Dyes Pigm.*, **95**, 112–115 (2012).
9. H. D. Li, L. L. Li, B. Z. Yin, *Inorg. Chem. Commun.*, **42**, 1–4 (2014).
10. B. D'Autre aux, N. P. Tucker, R. Dixon, S. Spiro, *Nature*, **437**, 769–772 (2005).
11. J. W. Lee, J. D. Helmann, *Nature*, **440**, 363–367 (2006).
12. G. Li, F. R. Tao, H. Wang, Y. C. Li, L. P. Wang, *Sens. Actuators B*, **211**, 325–331 (2015).
13. S. Das, K. G. Thomas, K. J. Thomas, V. Madhavan, D. Liu, P. V. Kamat, M. V. J. George, *Phys. Chem.*, **100**, 17310–17315 (1996).
14. M. Formica, V. Fusi, L. Giorgi, M. Micheloni, *Coord. Chem. Rev.*, **256**, 170–192 (2012).
15. J. L. Bricks, A. Kovalchuk, C. Trieflinger, M. Nofz, M. B schel, A. I. Tolmachev, J. Daub, K. Rurack, *J. Am. Chem. Soc.*, **127**, 13522–13529 (2005).
16. Y. Xiang, A. Tong, *Org. Lett.*, **8**, 1549–1552 (2006).